waves, we need precise corrections for complex path effects, source location, focal mechanisms, site conditions, and so on in order to get such a diagram. With coda waves, we have only to take spectral ratios for two different earthquakes with a station, because coda waves, unlike other kinds of seismic waves, represent the average characteristics of site, path and source effects.

These examples are particularly important for a) the corner frequency as a function of magnitude because the corner frequency is proven to be related to the stress drop of earthquake faulting, but is very difficult to estimate for small earthquakes, and b) high frequency spectra radiated by large earthquakes because paths, locations, and source mechanism effects become extremely complex in such a case, owing to large fault sizes. Although we still cannot give clear answers to the above two questions, coda waves will definitely give much more reliable values than direct waves.

### (e) Temporal Variation of Coda $Q$

There have been several reports of coda $Q$ values changing before and after large earthquakes. One very clear example was found in an eruption of Mt. St. Helens in Washington, U.S.A. Coda waves before several eruptions decayed in time much more strongly than after the eruptions (Fig. 2.26). This change is probably due to the opening and closing of microfractures around the volcanic body by stress enchancement coinciding with magma movement. In the case of earthquakes, it is hard to show any evidence as clear as in volcanic eruptions, but several similar phenomena have been found such as the coda Q change before and after the Tangshan, China, earthquake in 1976 (Fig.2.27). However, more careful observations will be required in order to use this phenomenon as a precursor of large earthquakes.

## 2.2 Fluctuation of Amplitude and Phase Observed by Seismic Arrays

In this chapter, we shall consider amplitude and phase fluctuations observed by seismic arrays with teleseismic events. We assume that a wave incident from below is coherent in the bottom of the lithosphere and only velocity perturbations in the lithosphere cause the above fluctuations. The fluctuations are considered to be random and no back-scattering contributes such fluctuations (Fig. 2.28).

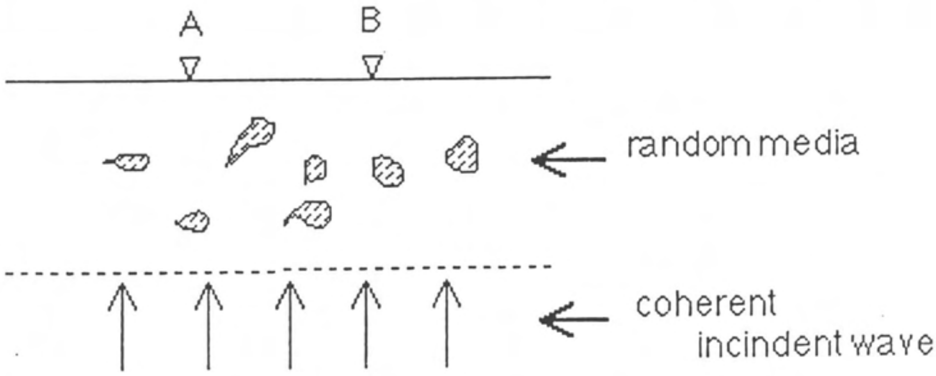


Fig. 2.28: Teleseismic array observation for lithosphere as random media.

We apply the theory of Chernov (1960) on random media, based on the Born approximation explained below. The principal idea for "randomness" is as follows: the cross-correlation of observations between stations $A$ and $B$ is a function only of the distance between these two stations and propotional to its distance. Fig. 2.29 gives one of such an array observations taken from Aki (1973) with the LASA array in Montana, U.S.A.

The figures give array configurations, observed seismograms for teleseismic events, and azimuthal variations of observed fluctuations of amplitude and phase delay. The Chernov theory is based on the Born

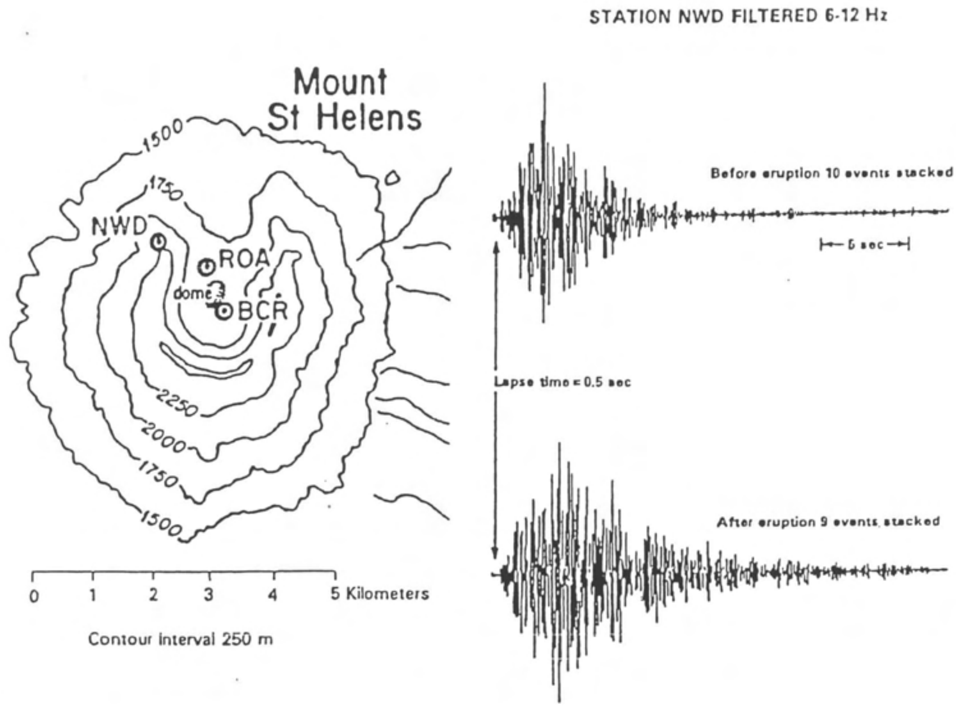


Fig. 2.26: Stacked seismograms recorded at near-summit stations before and after an eruption of Mt. St. Helens [Fehler et at., 1988]. (Copyright by the American Geophysical Union)

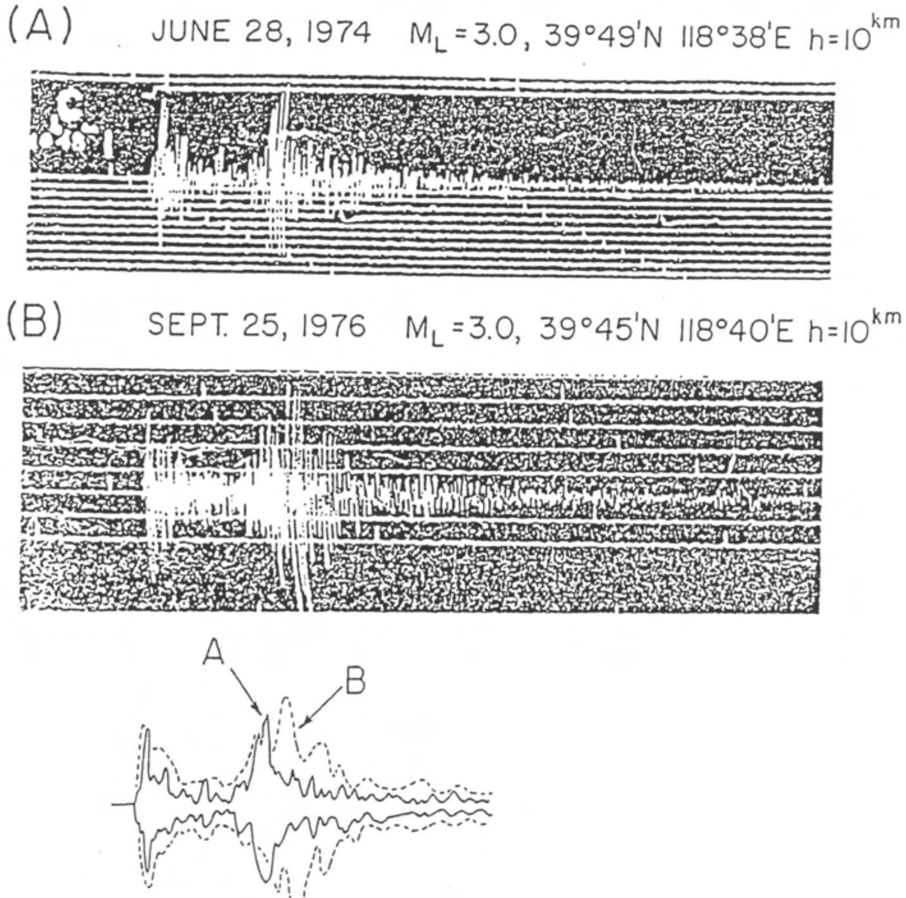


Fig. 2.27: Vertical seismograms recorded for local earthquakes before and after the Tangshan, China, earthquake in 1976 [Jin and Aki, 1986]. (Copyright by the American Geophysical Union)

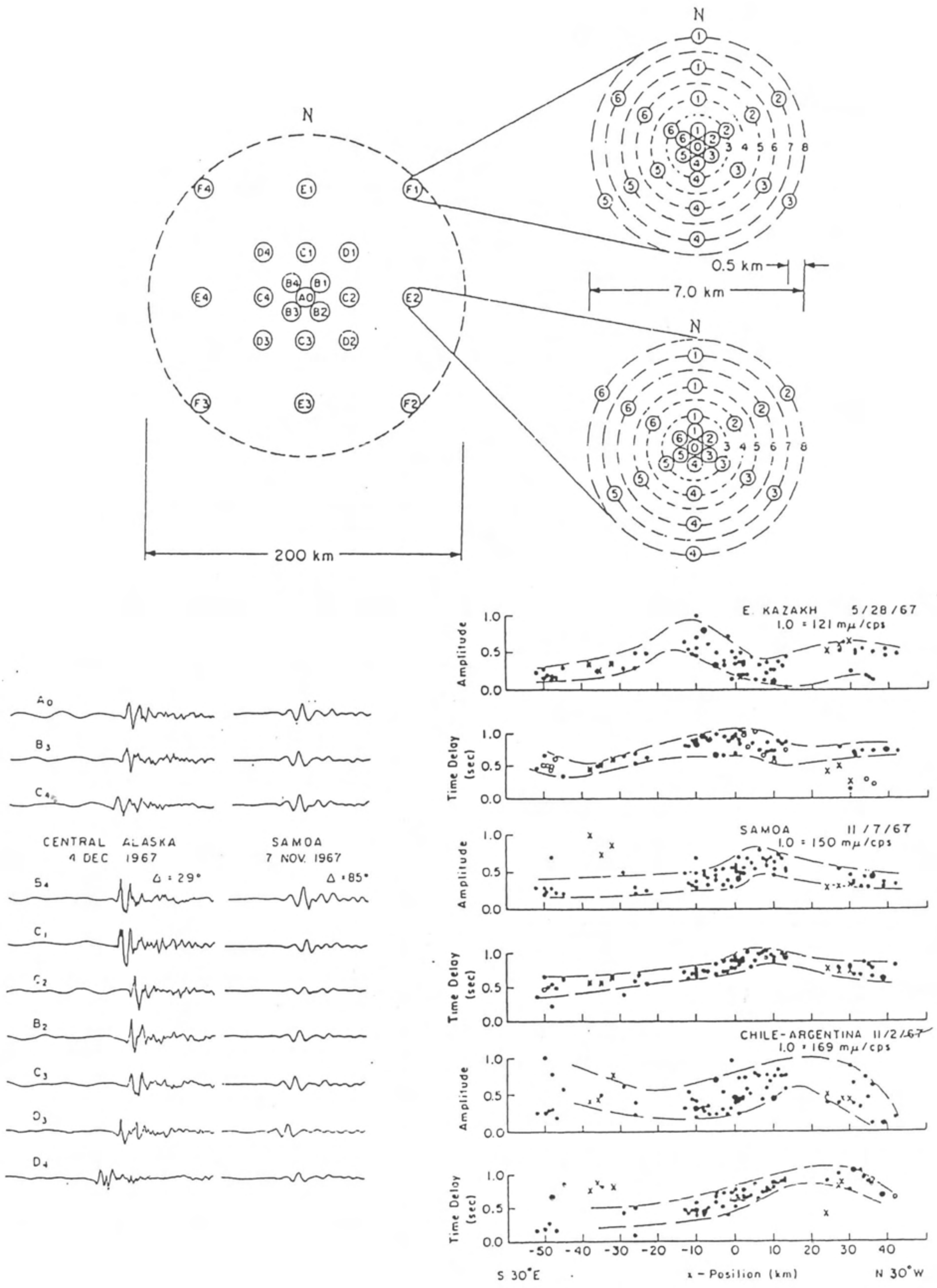


Fig. 2.29: Configuration of the LASA array, teleseismic seismograms, and variation in phase delay and amplitude within the array for different events [Aki, 1973]. (Copyright by the American Geophysical Union)

variations of observed fluctuations of amplitude and phase delay. The Chernov theory is based on the Born scattering or weak scattering theory. Under such an assumption that, if velocity perturbation is negative, the arrival time of one specific seismic phase is delayed (i.e., positive phase delay) and its amplitude becomes large, and vice versa for positive velocity perturbation. Such a tendency can be observed in most correlation diagrams observed between phase delay and amplitude anomalies. We therefore judge that the application of the Chernov theory would be valid with most teleseismic observations.

Now let us briefly explain the theory applicable to our problem. Although we are currently dealing with seismic waves or elastic waves, we adopt the scalar wave assumption, and our wavefield $\Phi(\mathbf{x}, t)$ satisfies the scalar wave equation:

$$\frac{\partial^2 \Phi}{\partial t^2} = \alpha^2(\mathbf{x}) \nabla^2 \Phi$$

where $\alpha(\mathbf{x})$ gives the velocity as a spatial function $\mathbf{x}$. This assumption means that we neglect any conversion of waves such as a P-S conversion, which is usually valid of the present kind of observations. Here we introduce a small velocity fluctuation as

$$\alpha(\mathbf{x}) = \alpha_0 \delta\alpha(\mathbf{x}), \quad \frac{\delta\alpha}{\alpha_0} \ll 1$$

where $\alpha_0$ is the constant reference velocity and $\delta\alpha(\mathbf{x})$ is the velocity fluctuation. Following the Born approximation, the above velocity fluctuation is supposed to yield the small fluctuation of the wavefield considered:

$$\Phi(\mathbf{x}, t) = \Phi^0(\mathbf{x}, t) + \Phi'(\mathbf{x}, t), \quad \Phi^0 \gg \Phi'$$

where $\Phi^0$ and $\Phi'$ are the primary wave field with the constant reference velocity $\alpha_0$ and the scattered wavefield caused by the velocity fluctuation $\delta\alpha$, respectively. The scalar wave equation thus becomes

$$\frac{\partial^2(\Phi^0 + \Phi')}{\partial t^2} = (\alpha_0 + \delta\alpha)^2 \nabla^2 (\Phi^0 + \Phi')$$

and we take only a few terms of a lower order. For the 0-th order,

$$\frac{\partial^2 \Phi^0}{\partial t^2} = \alpha_0^2 \nabla^2 \Phi^0$$

which describes the reference wavefield. For the 1-st order,

$$\frac{\partial^2 \Phi'}{\partial t^2} = \alpha_0^2 \nabla^2 \Phi' + 2\alpha_0 \delta\alpha \nabla^2 \Phi^0$$

which gives the equation governing the scattered wavefield $\Phi'$. This equation can be considered as a scalar wave equation for $\Phi'$ with an inhomogenous or source term $\chi(\mathbf{x}, t) \equiv 2\alpha_0 \delta\alpha \nabla^2 \Phi^0$, which gives the solution in the form of a retarded potential:

$$\Phi'(\mathbf{x}, t) = \frac{1}{4\pi\alpha^2} \iiint_V \frac{\chi(\xi, t - |\mathbf{x} - \xi| / \alpha_0)}{|\mathbf{x} - \xi|} dV(\xi).$$

We take a plane wave propagating in the $x_1$ direction as our incident wave, which is expressed by

$$\Phi^0(\mathbf{x},t) = A\exp\left[\frac{i\omega x_1}{\alpha_0} - i\omega t\right],$$

then the scattered wavefield is given by

$$\Phi'(\mathbf{x},t) = \frac{A\omega^2}{2\pi\alpha_0^2}\iiint_V\left(-\frac{\delta\alpha}{\alpha_0}\right)\frac{\exp[-i\omega(t - r/\alpha_0 - \xi_1/\alpha_0)]}{r}dV(\xi)$$

where $r = |\mathbf{x} - \xi|$ (Fig. 2.30). Our goal is not to get a deterministic solution of the above form, because in random media only statistically representative values have significance. We do not consider $\delta\alpha$ and $\Phi'$ themselves but their averaged values over space defined with $< >$. We take the autocorrelation function of velocity fluctuation $\mu(\mathbf{x}) \equiv -\delta\alpha/\alpha_0$:

$$<\mu(r')\,\mu(r'+r)> = <\mu^2> N(r)$$

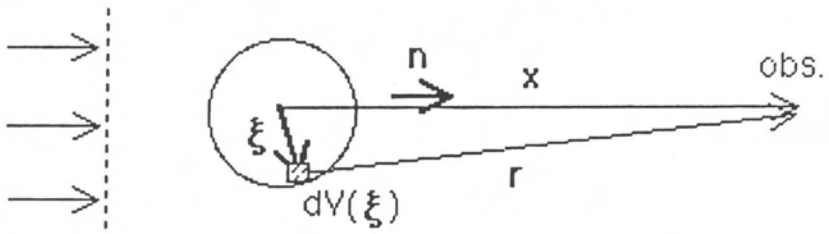


**Fig. 2.30: Weak scattering theory.**

with the normalization of $N(0) = 1$. Since the media are assumed to be random, $N$ depends only on the distance $r$ between two positions, and does not include any directional information. We only consider the function $N(r)$ in characterizing the properties of the media without taking care of the details of velocity fuctuation. As given in Appendix B, under the assumption of the observation points within the first Fresnel zone, $L^2/\lambda|\xi| \ll 1$, where $L$ is the travel distance, $\lambda$ is the wavelength considered, and $|\xi|$ is the typical size of scatterers, the variance of wavefield fluctuations is expressed by

$$<|\Phi'|^2> = \frac{A^2k^4 <\mu^2> V}{4\pi^2|\mathbf{x}|^2}4\pi\int_0^\infty N(r')\frac{\sin(k|\mathbf{K}|r')}{k|\mathbf{K}|}r'\,dr'$$

where $k$ is the wavenumber and $\mathbf{K}$ is the polar axis vector in the direction of the incident wave. The above equation gives our final solution or expresses the relation between the scattered wavefield $<|\Phi'|^2>$ and the random media $N(r)$.

Following Chernov (1960), we consider random media characterized by the following two forms of $N(r)$:

1. $N(r) = e^{-|r|/a}$ ($a$ : autocorrelation distance) (Fig.2.31)
   Then, the above relation is expressed by

$$<|\Phi'|^2> = \frac{A^2k^4 <\mu^2> a^3 V}{\pi|\mathbf{x}|^2}\left(1 + 4k^2a^2\sin^2\frac{\theta}{2}\right)^{-2}$$

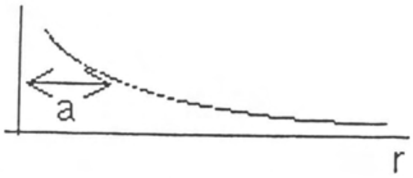


**Fig. 2.31: Exponential type of autocorrelation function.**

2. $N(r) = e^{-|r|^2/a^2}$ (Fig. 2.32)

$$<|\Phi'|^2> = \frac{A^2k^4 <\mu^2> a^3V}{4\sqrt{\pi}|\mathbf{x}|^2}\exp\left(-k^2a^2\sin\frac{\theta}{2}\right).$$


**Fig. 2.32: Gaussian type of autocorrelation function**

where $\theta$ is the angle between the direction of the primary wave (i.e., the $x_1$ axis) and the observation point.

Let us consider high and low frequency limits of the above results in order to interpret their physical meanings.

- $ka = 2\pi\alpha / \lambda \rightarrow 0$: long wave approximation, it then gives

$$<|\Phi'|^2> \propto k^4.$$

The scattered wavefield is very weak and does not depend on its azimuth $\theta$, or in other words, the scattering is isotropic. This type of scattering is called the Rayleigh scattering that Lord Rayleigh studied for the scattering of sunlight by the air thus producing the blue sky.

- $ka \rightarrow$ large: short wave approximation

Scattered energy is concentrated in the forward direction or the direction of the incident wave propagating. The characteristic angle of the concentration of its energy is $\theta \sim (ka)^{-1}$, which means that scattered waves are focused, or the heterogeneities act as if they were mirrors, producing a clear shadow (Fig.2.33).

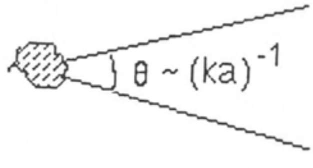


**Fig. 2.33: Shadow produced by a scatterer with short wave approximation.**

We finally apply the above results to the data recorded at LASA. We neglect the surface effect so that the above formulations with unbounded random media may be used. It is apparent that the wave incident to the bottom of the lithosphere below the array is defined as a plane wave $\Phi^0$ and heterogeneities in the lithosphere below produce scattered waves $\Phi'$ (Fig.2.34). Our data set consists of the following statistically representative

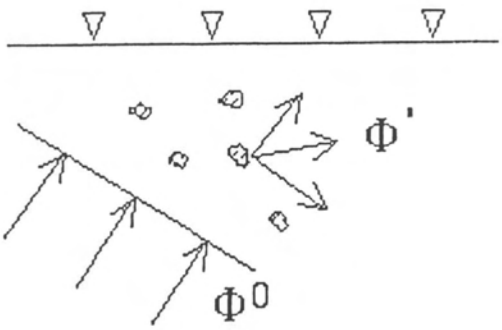


Fig. 2.34: Incident $\Phi^0$ and scattered $\Phi'$ wavefields.

$$<(\Delta\phi)^2> \equiv \sigma_\phi^2,$$
$$<(\Delta \ln A)^2> \equiv \sigma_A^2.$$

Note that $\Delta\phi/\omega$ corresponds to the travel time anomalies usually used in studies on heterogeneities within the earth. Next, we take autocorrelations and crosscorrelation of $\Delta\phi$ and $\Delta \ln A$ :

$$<\Delta\phi(x)\cdot\Delta\phi(x+X)> \equiv f_\phi(X),$$
$$<\Delta \ln A(x)\cdot\Delta \ln A(x+X)> \equiv f_A(X),$$
$$<\Delta \ln A\cdot\Delta\phi> \equiv \rho\sigma_\phi\sigma_A$$

where $\rho$ is the correlation coefficient between a phase delay and an amplitude anomaly.

Fig.2.35 shows the autocorrelations of observed phase delays and amplitude anomalies as a function of distance in the two frequency ranges and with several incident directions or earthquakes at different locations. The form of these autocorrelation functioning with respect to the distance gives the type of random media, and in this case, the $N(r)=e^{-|r|^2/a^2}$ type mentioned above fits the data better than other models. Phase fluctuation is correlated better even at long distance than with amplitude fluctuation. In other words, phase fluctuation can be said to be spatially smoother. The correlation scales of both variables give the estimate of the correlation distance $a$ in the medium. Using the magnitude of the crosscorrelation coefficient $\rho$, we further estimate the value of $L$, which is the extent of the heterogeneous region causing fluctuations in data observed across the array. Finally, the magnitudes of autocorrelations $\sigma_\phi$ and $\sigma_A$ give the estimate of the absolute mean values of velocity fluctuation in the medium.

Following the comparison in data with model predictions as described above, the LASA observation can be summarized as follows:

1. The randomness is characterized well by $N(r)=e^{-|r|^2/a^2}$ from the shape of the autocorrelation functions.
2. The correlation scale of the autocorrelation functions gives the correlation distance of velocity fluctuation in the lithosphere of this area to be $a \simeq 10$ km.
3. The crosscorrelation coefficient $\rho$ is related to the wave parameter $D = 2\lambda L/\pi a^2$, which is about 5 in the present case. We can then estimate $L \sim 60$ km, which corresponds to the extent of the heterogeneous region.

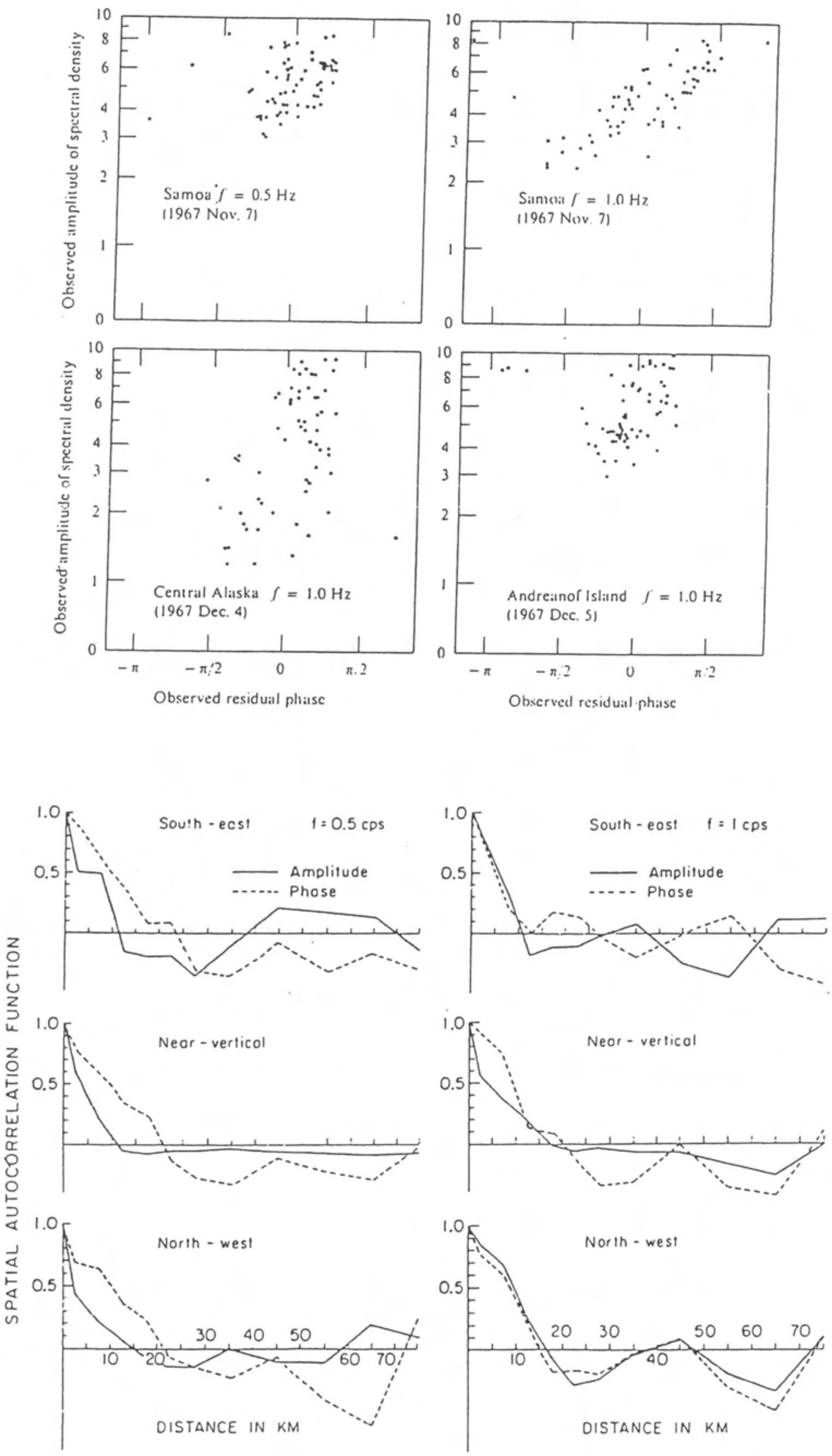


Fig. 2.35: Relationship between phase delay and amplitude observed at LASA for P waves for four events, and spatial autocorrelations with different incident directions [Aki, 1973]. (Copyright by the American Geophysical Union)

geneous region.

4. Once we get the above values, we can estimate the average magnitude of velocity fluctuation in the medium from the variances of phase delay and amplitude anomaly. In this case, $\sqrt{<\mu>^2} \simeq 4\%$

It should be very important to apply this kind of statistical approach in many areas, because any deterministic studies such as travel time inversion or tomography cannot be applied in the high frequency range and they only give maps of heterogeneities after smoothing out much finer and stronger heterogeneities. We must always remember that such maps only give partial information on the heterogeneities in the earth and there should be much more complex heterogeneities in the actual earth.

**Appendix A: Derivation of Coda Decay Formulation with the Single Scattering Model**

In this appendix, we shall derive a coda decay formulation based on the single scattering model. Let us assume that our source and receiver are located at a same point, and that the coda part consists of wave scattered only once by a heterogeneity or a scatterer distributed randomly over our model space (Fig.2.36).

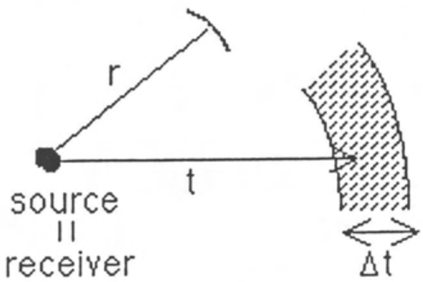


**Fig. 2.36: Configuration of single scattering theory.**

First, we define the following two functions in frequency domain $\omega$,

$\phi(\omega \mid r_n)$ : Fourier tranform of a back-scattered wavelet from the $n$-th scatterer located at $r_n$

$f(\omega \mid t)$ : Fourier tranform of coda waves filtered by the time window $(t - \Delta t/2, t + \Delta t/2)$

Then, the coda wave is defined as an ensemble of waves scattered by each scatterer as follows:

$$f(\omega|t) = \sum_n \phi(\omega|r_n), \qquad r - \frac{\Delta r}{2} < r_n < r + \frac{\Delta r}{2}$$

summing up all the scatterers in the defined area. The area corresponds to $t = 2r/\beta$ or the round trip time from the source to a scatterer. This expression means that scattered wavefields are indepedent or random, or in other words, there is no correlation among scatterers.

Consider the power spectrum of coda waves represented as a stochastic process:

$$E\left\{\left|\sum_n \phi(\omega|r_n)\right|^2\right\} = \sum_n \sum_{n'} E\{\phi(\omega|r_n)\phi^*(\omega|r_{n'})\}$$
$$= \sum_n E\{|\phi^2(\omega|r_n)|\}$$

where $E$ represents the expectation value of a given function. The above formulation is derived because scattered wavefields are uncorrelated or independent among scatterers. The power spectrum of coda waves then defined as

$$P(\omega|t) = \sum_n E\left\{|\phi(\omega|r_n)|^2\right\} / \Delta t$$

where $r - \Delta r /2 < r_n < r + \Delta r/2$. Assuming that all the scatterers have identical effects (i.e., randomness in media is homogeneous), the scattered wavefield does not depend on a specific scatterer:

$$\phi(\omega | r_n) = \phi(\omega | r).$$

Defining $N(r)$ as the total number of scatterers within the radius $r$ from the source, we can write the summation in the above formulation as

$$\begin{aligned} P(\omega|r) &= \frac{dN}{dr}\frac{\Delta r}{\Delta t}|\phi(\omega|r)|^2 \\ &= \frac{\beta}{2}\frac{dN}{dr}|\phi(\omega|r)|^2 \end{aligned}$$

with $\Delta t = 2\Delta r / \beta$. Apart of the coda waves between $t$ and $t + \Delta t$ is considered to be contributed from waves scattered by heterogeneities in a spherical shell region between $r$ and $r + \Delta r$ (Fig.2.37).

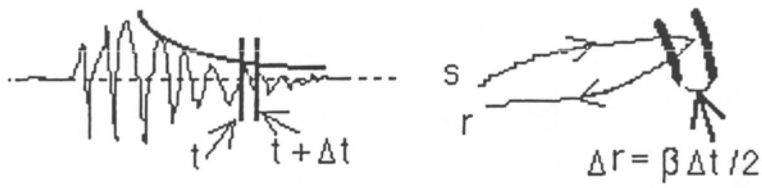


**Fig. 2.37: Coda part and corresponding region with scatterers.**

Next, we define the scattering coefficient $g(\theta)$ as the fractional loss of energy by scattering in the solid angle $d\Omega$ around $\theta$-direction per unit travel distance of the primary plane wave $A_0\exp(i\omega(x/\beta-t))$ (for example, refer to Goldstein, "Classical Mechanics", § 3-10 or Landau and Lifshitz, "Mechanics", § 18), as shown in Fig.2.38.

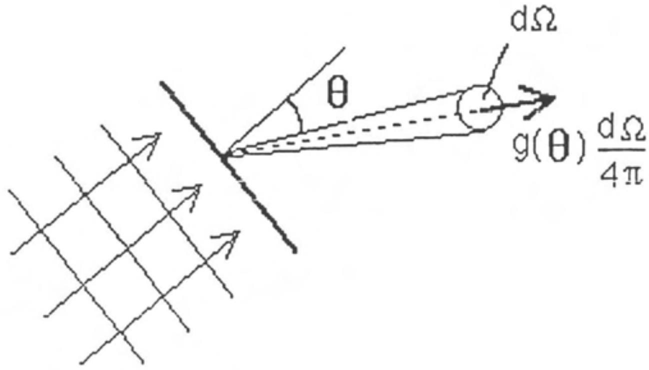


Fig. 2.38: Scattering coefficient $g(\theta)$.

We then consider energy content of both incident and scattered waves (Fig.2.39).

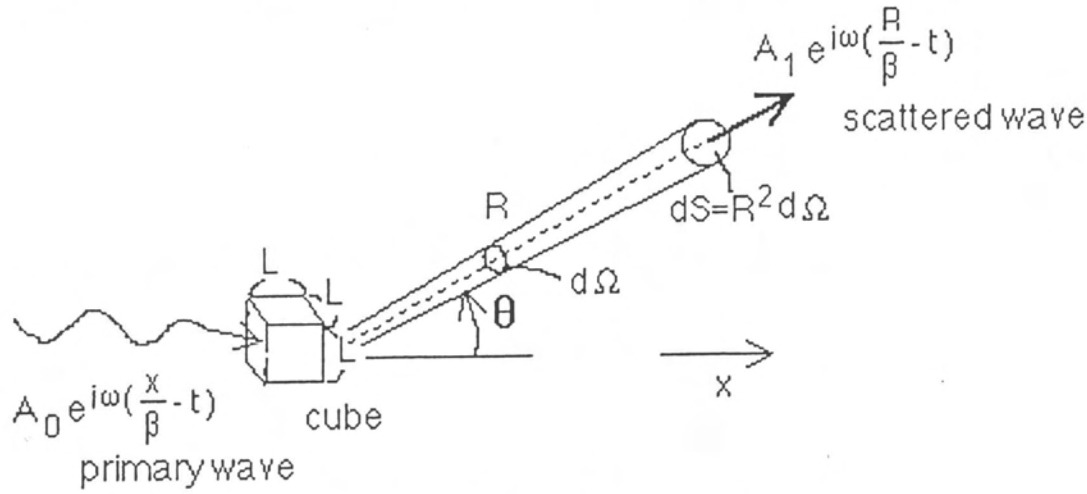


**Fig. 2.39: Primary and scattered waves.**

$$[\text{incident wave energy}] = A_0^2 L^2 \times \text{const.}$$

where the constant depends on medium properties, frequency, and so on. This means that wave energy is proportional to the cross section of the heterogeneous region. Meanwhile, the energy loss due to scattering is balanced with the scattered energy as follows:

$$L \times \frac{g(\theta)}{4\pi} \times A_0^2 L^2 \times \text{const.} = \text{const.} \times A_1^2 R^2 d\Omega,$$

where the first $L$ represents the thickness of the heterogeneous region. We therefore obtain

$$A_1^2 = A_0^2 \frac{g(\theta) L^3}{4\pi R^2}$$

where the volume of scatterers $L^3 = 4\pi R^2 \Delta r$. Since these amplitudes correspond to the incident wave $A_0 = |\phi_0(\omega | r)|$ and the scattered wave $A_1 = |\phi(\omega | r)|$ as defined before, the coda power spectrum may become

$$\begin{aligned} P(\omega|t) &= \frac{\beta}{2}\frac{dN}{dr}|\phi(\omega|r)|^2 = \frac{\beta}{2}\frac{|A_1|^2}{\Delta r} \\ &= \frac{\beta|A_0|^2}{2\Delta r}\frac{g(\pi)4\pi R^2 \Delta r}{4\pi R^2} = \frac{\beta}{2} g(\pi)|\phi_0(\omega|r)|^2 \end{aligned}$$

by simplifying $\Delta N = 1$. $g(\pi)$ represents the back-scattered wave with $\theta = \pi$ or the energy scattered straight back. We can finally express the coda spectrum as

$$P(\omega|t) = \frac{\beta}{2} g(\pi)|\phi_0(\omega|r)|^2$$

with $r = \beta t/2$.

Assuming that both the primary and scattered waves attenuate as they propagate with the rate of $Q_c$ in the actual earth, the above formulation may be modified as

$$P(\omega|t) = \frac{\beta}{2} g(\pi) \left| \phi_0(\omega | \frac{\beta t}{2}) \right|^2 e^{-\omega t/Qc}.$$

Since the wavefront of the incident wave spreads out three-dimensionally or $\phi_0(\omega \mid r) \sim 1/r$ with $t = 2r/\beta$,

$$P(\omega|t) \propto \frac{1}{t^2} e^{-\omega t/Qc}.$$

For surface waves, on the other hand, $\phi_0(\omega|r) \sim \frac{1}{\sqrt{r}}$. We therefore get

$$P(\omega|t) \sim \frac{1}{t} e^{-\omega t/Qc}.$$

Thus, we can write the term of coda wave spectrum indepent of source and receiver ingeneral as

$$C(\omega \mid t) = Bt^{-m} e^{-\omega t/Qc}$$

where $B$ is a constant, and $m \simeq 2$ for body waves.

## Appendix B: Averaged Scattered Wavefield as a Function of Autocorrelation of Velocity Fluctuations

In this appendix, we shall derive the relationship between the variance of scattered wavefields $<|\Phi'|^2>$ and the autocorrelation function of velocity fluctuation $N(r)$, which was omitted in the main text. We start with the formulation:

$$\Phi'(\mathrm{x},t) = \frac{A\omega^2}{2\pi\alpha_0^2} \iiint_V \left(-\frac{\delta\alpha}{\alpha_0}\right) \frac{\exp[-i\omega(t - r/\alpha_0 - \xi_1/\alpha_0)]}{r} dV(\xi)$$

where $r = |\mathrm{x} - \xi|$. This will be connected with the autocorrelation function $N(r)$ defined by $\mu(\mathrm{x}) \equiv -\delta\alpha/\alpha_0$ as follows:

$$<\mu(r')\mu(r'+r)> = <\mu^2> N(r)$$

with $N(0) = 1$.

Under the assumption that we only consider scattered wavefields inside the first Fresnel zone $L^2/\lambda|\xi| \ll 1$,

$$\begin{aligned} r &= (|\mathrm{x}|^2 + |\xi|^2 - 2\mathrm{x}\cdot\xi)^{1/2} \\ &\sim |\mathrm{x}| - \mathbf{n}\cdot\xi, \end{aligned}$$

where $\mathbf{n}$ is the unit vector in the direction of $\mathbf{x}$. Then, the above equation may be written as

$$\Phi'(\mathrm{x},t) \simeq \frac{Ak^2 \exp[-i(\omega t - k|\mathrm{x}|)]}{2\pi|\mathrm{x}|} \int_V \mu(\xi) \exp[ik(\xi_1 - \mathbf{n}\cdot\xi)] dV(\xi).$$

We do not deterministically evaluate the above value but some statistical values such as the variance of $\Phi'$,

$$
\begin{aligned}
<|\Phi'(\mathbf{x},t)|^2> &= <\Phi'(\mathbf{x},t)\Phi'^*(\mathbf{x},t)> \\
&\simeq <\frac{A^2k^2}{(2\pi|\mathbf{x}|)^2}\int_V\int_{V'}\mu(\xi)\mu(\xi')\exp\{ik(\xi_1-\xi_1'-\mathbf{n}\cdot(\xi-\xi'))\}dV(\xi)dV(\xi')> \\
&\simeq \frac{A^2k^2}{4\pi^2|\mathbf{x}|^2}\int_V\int_{V'}<\mu(\xi)\mu(\xi')>\exp\{ik(\xi_1-\xi_1'-\mathbf{n}\cdot(\xi-\xi'))\}dV(\xi)dV(\xi').
\end{aligned}
$$

This equation means sending a wave in a random medium and averaging observations over many receivers over the model. Taking $\mathbf{e}_1$ as the unit vector along $x_1$ or the direction of the incident wave and $\theta$ as the angle between the observation and the incident wave direction (Fig.2.40), we define the vector as

$$\mathbf{K} \equiv \mathbf{e}_1 - \mathbf{n},$$

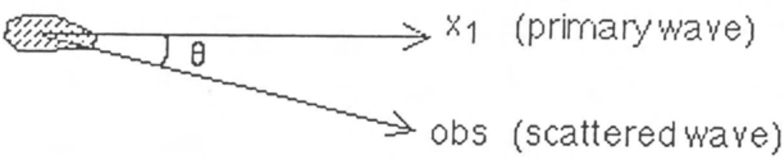


**Fig. 2.40: Angle between primary and scattered waves.**

then the cosine theorem gives

$$|\mathbf{K}|^2 = 1+1-2\cos\theta = 4\sin^2\frac{\theta}{2}.$$

Furthermore, since $\xi_1 - \xi'_1 = \mathbf{e}_1 \cdot (\xi - \xi')$, the exponential part of the above equation becomes $\exp\{ik\mathbf{K}\cdot(\xi-\xi')\}$ with $k = \omega/\alpha_0$.

Chernov (1960) introduced the following new coordinate system to evaluate the integrations in the above formulation:

$$
\begin{cases}
\hat{\xi} \equiv \xi - \xi' & \text{:relative coordinate} \\
\bar{\xi} \equiv (\xi + \xi')/2 & \text{:center-of-mass coordinate}
\end{cases}
$$

the integrations are then expressed by the new coordinate system:

$$dV(\xi)dV(\xi') = d\xi_1 d\xi_2 d\xi_3 d\xi_1' d\xi_2' d\xi_3' \rightarrow d\hat{\xi}_1 d\hat{\xi}_2 d\hat{\xi}_3 d\bar{\xi}_1 d\bar{\xi}_2 d\bar{\xi}_3$$

because the Jacobian of the present coordinate transformation is one. Assuming that statistical vairables in the present case do not depend on its position (i.e., stationary in space), which means

$$\int_V d\bar{\xi}_1 d\bar{\xi}_2 d\bar{\xi}_3 = V,$$

our formulation may become

$$<|\Phi'(\mathbf{x},t)|^2>=\frac{A^2k^4<\mu^2>V}{4\pi^2|\mathbf{x}|^2}\int_V N(\hat{\xi})\exp(ik\mathbf{K}\cdot\hat{\xi})d\hat{\xi}_1 d\hat{\xi}_2 d\hat{\xi}_3.$$

Our final procedure is to evalutate the above integrations by transforming to the spherical coordinate system:

$$(\hat{\xi}_1,\hat{\xi}_2,\hat{\xi}_3)\rightarrow(r',\theta',\phi')$$

where the polar axis corresponds to **K** or the direction of the incident wave. It is obvious (Fig. 2.40) that

$$r'=|\hat{\xi}|,$$
$$\mathbf{K}\cdot\hat{\xi}=|\mathbf{K}|r'\cos\theta',$$
$$d\hat{\xi}_1 d\hat{\xi}_2 d\hat{\xi}_3=r'\sin\theta' dr' d\theta' d\phi'.$$

Since the integration over $\theta'$ and $\phi'$ in our formulation is done as

$$\int_0^{\pi}\exp(iB\cos\theta')\sin\theta' d\theta'=\frac{\exp(-iB)-\exp(iB)}{-iB}=2\frac{\sin B}{B}$$

and

$$\int_0^{2\pi}d\phi'=2\pi,$$

we obtain the following final relation between the variance of a scattered wavefield and the autocorrelation function of velocity fluctuations:

$$<|\Phi'|^2>=\frac{A^2k^4<\mu^2>V}{4\pi^2|\mathbf{x}|^2}4\pi\int_0^{\infty}N(r)\frac{\sin(k|\mathbf{K}|r')}{k|\mathbf{K}|}r' dr'.$$

Here we assume $N(\hat{\xi})=N(|\hat{\xi}|)$ or the autocorrelation is a function only of the distance but not the azimuth, which means that we use an isotropically random medium.

# References

## PART II


Aki., K., Analysis of the seismic coda of local earthquakes as scattered waves, *J. Geophys. Res.*, *74*, 615-631, 1969.

Aki, K., Scattering of P waves under the Montana Lasa, *J. Geophys. Res.*, *78*, 1334-1346,1973.

Aki., K. and B. Chouet, Origin of coda waves: Source, attenuation, and scattering effects, *J. Geophys. Res.*, *80*, 3322-3342, 1975.

Aki, K., and P. G. Richards, *Quantitative Seismology: Theory and Methods*, p728-751, W.H. Freeman, San Francisco, 1980.

Chernov, L.A., *Wave propagation in a random medium*, McGraw-Hill, New York, pp. 168, 1960.

Fehler, M., P. Roberts, and T. Fairbanks, A temporal change in coda wave attenuation observed during an eruption of Mt. St. Helens, *J. Geophys. Res.*, *93*, 4367-4373, 1988.

Herraiz, M. and A.F. Espinosa, Coda Waves: A review, *Pure Appl. Geophys.*, *125*, 499-577, 1987.

Hoshiba, M., and K. Goto, Regional variation of seismic attenuation in the Japanese Island, *Prog. Abs. Seismol. Soc. Japan* (in Japanese), *1*, 85, 1988.

Jin, A. and K. Aki, Temporal change in coda Q before the Tanshang earthquake of 1976 and the Haicheng earthquake of 1975, *J. Geophys. Res.*, *91*, 665-673, 1986.

Lamb, H., On the propagation of tremors over the surface of an elastic solid, *Phil. Trans. Roy. Soc. London*, *A203*, 1-42, 1904.

Phillips, W.S., and K. Aki, Site amplification of coda waves from local earthquakes in central California, *Bull. Seismol. Soc. Amer.*, *76*, 627-648, 1986.

Rautian, T.G., V.I. Khalturin, The use of coda for determination of the earthquake source spectrum, *Bull. Seismol. Soc. Amer.*, *68*, 923-948, 1978.

Scheimer, J. and T.E. Landers, Short-period coda of a local event at LASA, Seismic Discrimination, *Semiannu. Tech. Sum. 42*, Lincoln Lab., Mass. Inst. of Technol., Cambridge, 1974.

Singh, S.K., and R.B. Hermann, Regionalization of crustal coda Q in the continental United States, *J. Geophys. Res.*, *88*, 527-538, 1983.

Tsujiura, M., Spectral analysis of the coda waves from local earthquake, *Bull. Earthquake Res. Inst.*, *53*, 1-48, 1978.

Wu, R.S., Seismic wave scattering, in *Encyclopedia of Solid Earth Geophysics*, ed. by D.E. James, Van Nostrand Reinhold, New York, 1166-1187, 1989.